CONDENSED MATTER PHYSICS

# Majorana-fermion origin of the planar thermal Hall effect in the Kitaev magnet α-$RuCl_3$

**Kumpei Imamura[1]†, Shota Suetsugu[2]†, Yuta Mizukami[1,3], Yusei Yoshida[1], Kenichiro Hashimoto[1], Kenichi Ohtsuka[2], Yuichi Kasahara[2], Nobuyuki Kurita[4], Hidekazu Tanaka[5], Pureum Noh[6], Joji Nasu[3], Eun-Gook Moon[6], Yuji Matsuda[2], Takasada Shibauchi[1]***



**The field-induced quantum-disordered state of layered honeycomb magnet α-$RuCl_3$ is a prime candidate for Kitaev spin liquids hosting Majorana fermions and non-Abelian anyons. Recent observations of anomalous planar thermal Hall effect demonstrate a topological edge mode, but whether it originates from Majorana fermions or bosonic magnons remains controversial. Here, we distinguish these origins from combined low-temperature measurements of high-resolution specific heat and thermal Hall conductivity with rotating magnetic fields within the honeycomb plane. A distinct closure of the low-energy bulk gap is observed for the fields in the Ru-Ru bond direction, and the gap opens rapidly when the field is tilted. Notably, this change occurs concomitantly with the sign reversal of the Hall effect. General discussions of topological bands show that this is the hallmark of an angle rotation–induced topological transition of fermions, providing conclusive evidence for the Majorana-fermion origin of the thermal Hall effect in α-$RuCl_3$.**

## INTRODUCTION

Majorana particles are fermions that are their own antiparticles. The realization of Majorana fermions as quasiparticles, which describe the excitations from the ground state in quantum materials, is at the forefront of condensed matter physics. In particular, enormous efforts have been devoted to the search for the Majorana bound states using superconductors and their topological hybrid systems (*1*), which are thought to be the first step toward topological quantum computing based on Majorana-based non-Abelian anyons. A totally different approach to the Majorana physics is the exactly solvable Kitaev model for insulating honeycomb magnets with bond-dependent Ising-type magnetic interactions, in which the ground state is a Kitaev spin liquid (KSL) (*2*). The excitations from the KSL ground state can be described by the itinerant Majorana fermions and $Z_2$ fluxes (or visons), which can be viewed as a fractionalization of the spins (*3*).

The Kitaev interactions, in which three bonds connected to a honeycomb lattice point have orthogonal Ising spin directions, have exchange frustration, leading to the KSL ground state. Such frustrated interactions can appear through the Jackeli-Khaliullin mechanism (*4*) in real materials having edge-sharing octahedra surrounding magnetic ions. One of the prime candidates for these Kitaev magnets is a spin-orbit–assisted Mott insulator α-$RuCl_3$ with a layered honeycomb structure (Fig. 1A). Each $Ru^{3+}$ ion with effective spin-1/2 has three bonds, where a cancelation of interactions between the two shortest Ru-Cl-Ru 90° paths leads to Ising interactions with the spin axis perpendicular to the plane including these two paths. The existence of substantial ferromagnetic Kitaev interactions with the energy scale of ~5 meV has been reported by experiments in α-$RuCl_3$ (*5*). Unfortunately, however, non-Kitaev magnetic interactions such as Heisenberg and off-diagonal terms also exist, and at low temperatures below ~7 K, an antiferromagnetic order with a zigzag spin structure occurs in the absence of a magnetic field (*6*). The application of in-plane magnetic fields of $\gtrsim$8 T can suppress the zigzag order, leading to the transition to a field-induced quantum-disordered state with no magnetic ordering down to the lowest temperature (*7*, *8*).

Within this high-field spin-disordered state of α-$RuCl_3$, the half-integer quantization plateau of thermal Hall conductivity $\kappa_{xy}$, which corresponds to half of the quantum thermal conductance $K_0 = (\pi^2/3)(k_B^2/h)T$ for electrons, has been reported (*9*–*11*). The quantized Hall effect is a signature characteristic of the edge current of fermionic particles, and the quantization to a half-integer value $K_0/2$ implies the non-Abelian phase of matter with Majorana fermions having a half degree of freedom of electrons. Another remarkable feature in α-$RuCl_3$ is that a finite transverse temperature gradient is observed even when the magnetic field is applied parallel to the in-plane thermal current, namely, the emergence of anomalous planar thermal Hall effect (*12*). In addition, the sign of quantized thermal Hall conductivity changes when the in-plane field component is reversed without changing the out-of-plane component. These results can be explained by the topological properties of Majorana fermions characterized by the Chern number ±1, whose sign is directly related to the direction of the edge current and thus the sign of quantized $\kappa_{xy}$. The Chern number is determined by the field direction in the KSL (*2*), which is consistent with the thermal Hall conductivity results (*12*). However, it has been reported that the half-integer quantization has been seen in a limited temperature and field range which has slight sample dependence (*10*, *11*, *13*, *14*). Moreover, in some samples, the magnitude of thermal Hall conductivity $\kappa_{xy}$ does not reach $K_0/2$ (*14*–*17*).

Recent theoretical calculations show that the sign change of the thermal Hall effect can also be explained by topological magnons in a specific parameter range, while the quantization is not expected (*18*–*22*). Very recent measurements of thermal Hall conductivity have been reported unquantized $\kappa_{xy}$ in the high-field disordered

[1]Department of Advanced Materials Science, University of Tokyo, Kashiwa, Chiba 277-8561, Japan. [2]Department of Physics, Kyoto University, Kyoto 606-8502, Japan. [3]Department of Physics, Tohoku University, Sendai 980-8578, Japan. [4]Department of Physics, Tokyo Institute of Technology, Meguro, Tokyo 152-8551, Japan. [5]Innovator and Inventor Development Platform, Tokyo Institute of Technology, Yokohama 226-8502, Japan. [6]Department of Physics, Korea Advanced Institute of Science and Technology (KAIST), Daejeon 34141, South Korea.
*Corresponding author. Email: shibauchi@k.u-tokyo.ac.jp
†These authors contributed equally to this work.

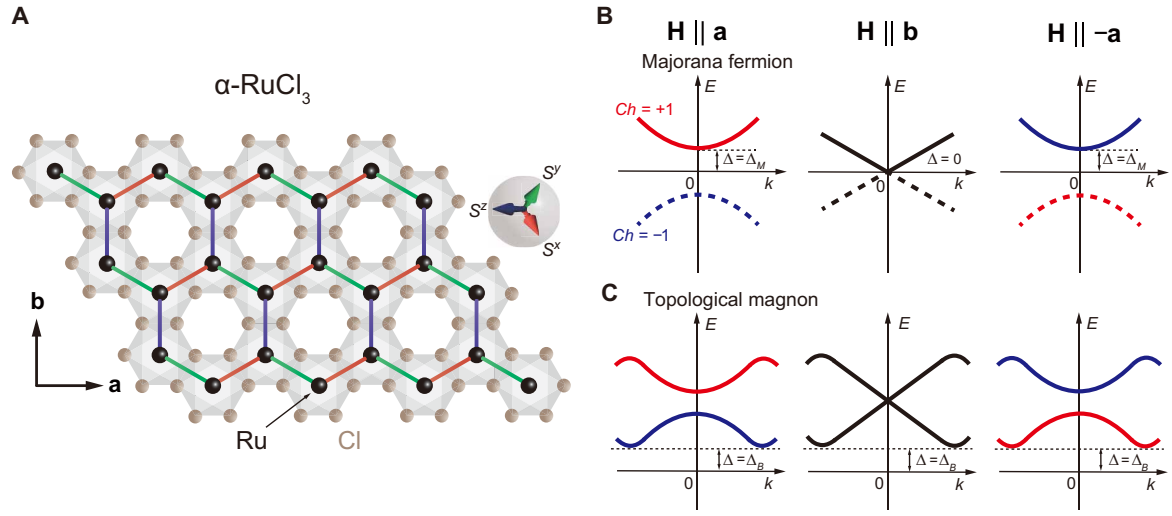


**Fig. 1. Key difference in the excitation spectra between Majorana fermions and topological magnons.** (**A**) Crystal structure of the honeycomb layer in α-$RuCl_3$. $Ru^{3+}$ ions (black circles) surrounded by octahedrons (shades) of $Cl^-$ ions (brown circles) form a layered honeycomb lattice. We define **a** and **b** axes perpendicular and parallel to the Ru-Ru bond direction (zigzag and armchair axes), respectively (left inset). [Here, we use the room-temperature *C*2/*m* notation of the crystal axes within the honeycomb plane (*36*).] The Ising spin axes $S^x$, $S^y$, and $S^z$ (right inset) are, respectively, perpendicular to the plane including the red, green, and blue Ru-Ru bond and the crossing shared edge of Cl octahedrons. (**B**) Schematic energy dispersion $E(k)$ of the itinerant Majorana fermions in a KSL. The red and blue curves have different topological Chern numbers +1 and −1, respectively. Note that the $E < 0$ part for the Majorana quasiparticle spectra are redundant (dashed lines), but its Chern number determines the topological properties. For field **H** parallel to the **a** (left) or −**a** axis (right), the Majorana excitations have a finite energy gap described by $\Delta_M$, which closes for **H**||**b** (middle). In other words, when the field angle is rotated, topological band crossing occurs at zero energy in the **b**-axis direction. (**C**) Similar plots for topological magnons. The band crossing occurs at a finite energy. In the spin-disordered phase, the lowest energy band, whose Chern number determines the topological properties, always has a finite gap $\Delta_B$.

state of α-$RuCl_3$, and it has been claimed that the behavior of $\kappa_{xy}(T)$ could be explained by the topological bosonic mode of magnons (*16*). It has also been suggested that a phonon Hall effect may be present and affect $\kappa_{xy}(T)$ in α-$RuCl_3$ (*17*). Thus, at the present stage, the variations in the $\kappa_{xy}$ data make it difficult to distinguish the origins, Majorana fermions, and bosons, only from the thermal Hall measurements in α-$RuCl_3$. In the bosonic scenario, $\kappa_{xy} \approx K_0/2$ would be just a coincidence. In the Majorana scenario, there are a few effects that can cause deviations of $\kappa_{xy}$ from $K_0/2$, including the phonon decoupling effect that can explain the temperature dependence (*23*, *24*) and the effect of partial cancelation due to twin domain formation that can account for the sample dependence of $\kappa_{xy}$ values (*25*). Under these circumstances, we need a different approach to distinguishing these origins without relying on the magnitude of $\kappa_{xy}$.

## RESULTS

Here, we point out that low-energy excitation spectra of Majorana fermions in the KSL and of topological magnons in the field-induced quantum disordered phase have essentially different field-angle dependence. This distinction between Majorana and magnon excitations is associated with the generic statistical difference that the Fermi energy is defined only for fermions and there are no negative-energy modes for bosons with zero chemical potential. In the Kitaev model (*2*), the Majorana excitation gap $\Delta_M \propto |M(\mathbf{H})|$ can be described by the mass function $M(\mathbf{H}) = \frac{h_x h_y h_z}{\Delta_{\mathrm{flux}}^2}$, which has characteristic dependence on the magnetic field $\mathbf{H} = (h_x, h_y, h_z)$ in the Ising spin axis coordinate. Here, $\Delta_{\mathrm{flux}}$ is the $Z_2$ flux gap whose energy scale should be larger than the Majorana gap $\Delta_M$ (*3*). We note that although the non-Kitaev interactions are present in α-$RuCl_3$, these interactions give $h_x + h_y + h_z$ terms in the mass function, which become zero for the fields within the honeycomb plane (*26*, *27*). As the spin axes are different from the crystallographic axes (Fig. 1A), we expect $\Delta_M \propto |\sin 3\phi|$ when we rotate the field within the honeycomb plane ($\phi$ is the field angle from the Ru-Ru bond direction). Therefore, the Majorana excitation spectrum has a finite gap for the field parallel to **a** or −**a** but it changes to gapless for **H**||**b**, as shown in Fig. 1B. The Chern number $Ch(\mathbf{H})$ is given by the sign of $h_x h_y h_z$, and it is +1 (−1) for **H**||−**a** (**H**||**a**) and 0 for **H**||**b** as **b**||[110] is perpendicular to the $S^z$ axis (see Fig. 1A). Thus, when the field is rotated within the plane, the sign change of $\kappa_{xy}$ occurs in the **b** direction ($\phi = 0°$), which should be accompanied by the gap closure, as manifested in the $h_x h_y h_z$ factor in the Chern number and the mass function. The closing of the gap for **H**||**b** is also a natural consequence of the $C_2$ rotational symmetry around the bond (armchair) axis (see the Supplementary Materials), when we focus on the irreducible representation for the idealized honeycomb layer with the point group $D_{3d}$ ($\bar{3}1m$) (*25*). In stark contrast, in the topological magnon case, the sign change of the Chern number of the lowest band is caused by the topological band crossing at finite energy, which is protected by the rule that the sum of the Chern integers for all positive magnon bands is zero (*28*). In this case, the change of the Chern numbers in magnon bands occurs even though the excitation gap does not close at zero energy (Fig. 1C). Thus, the topological transition between different Chern numbers, which can be induced by field-angle rotations, accompanies a complete closure

of low-energy excitation gap only for the Majorana fermion case (*27*, *29*).

From the above general arguments of topological bands, the key difference that can distinguish the two origins is whether the bulk low-energy excitations are gapless or gapped when the Chern number and the thermal Hall effect change sign in the bond direction (**H**||**b**). To test this experimentally, we combine low-temperature specific heat measurements for the bulk excitations and thermal Hall conductivity measurements for the edge currents in magnetic fields rotating within the honeycomb plane near the **b** direction. It should be emphasized that these thermal measurements are powerful and more direct probes of Majorana quasiparticles in the sense that they do not require the recombination of the fractionalized spins in the Kitaev material, unlike other spin excitation probes.

Figure 2A shows the field dependence of thermal Hall conductivity at several field angles ϕ defined as shown in Fig. 2B. In this single crystal, the half-integer quantization is seen in this field range of the quantum disordered phase with a positive (negative) sign for **H**||−**a** (**H**||**a**). For ϕ = −26°, $\kappa_{xy}/T \approx -0.5\ K_0/T$ shows a near quantization with an opposite sign from that for ϕ = −90° (**H**||−**a**), which is consistent with the sixfold sign reversals within the plane expected for the KSL (Fig. 2B). When the field angle ϕ is further rotated from negative to positive through ϕ = 0° (**H**||**b**), the sign of $\kappa_{xy}/T$ changes, which can be more clearly seen in Fig. 2C where the angular dependence of $\kappa_{xy}/T$ is shown at a fixed field of 11 T. These results indicate that the topological Chern number *Ch*, which determines the direction of the chiral edge current, changes its sign in the bond direction when the field is rotated within the honeycomb plane.

Having looked at the evidence from thermal transport measurements for the topological transition induced by field-angle rotation, we now turn to the low-energy excitation spectra in the bulk for **H**||**b**. We have developed a high-resolution, field-angle–resolved specific heat measurement system based on the long-relaxation technique (*26*), which can cover very low temperatures down to ~0.2 K that corresponds to ~1/300 of the Kitaev interaction by using a dilution fridge equipped with a two-axis piezo-based rotator (see the Supplementary Materials). In Fig. 3A, we show the raw data of low-temperature specific heat *C* without subtracting the phonon contribution, which is known to give a $C \propto T^3$ temperature dependence in this material (*26*, *30*). Thus, in this plot of $C/T^2$ versus *T*, the phonon contribution should be described by a linear slope with no intercept in the zero-temperature limit. The temperature dependence of $C/T^2$ for **H**||**b** shows a *T*-linear behavior, but with clear residual values for $T \to 0$ K in a wide-field range of the spin-disordered state. This indicates the presence of non-phononic low-lying excitations that are described by $C/T = \alpha T$, where α is a field-dependent coefficient. This is fully consistent with the gapless excitations of a Dirac cone-like dispersion ($E = v|\mathbf{k}|$) in a two-dimensional (2D) system, in which the coefficient α is proportional to the inverse of the square of the velocity *v*. This observation of gapless excitations for **H**||**b** contradicts the expected existence of a gap in the topological magnon case (Fig. 1C) and provides compelling evidence for the fermionic excitations in this system. We note that the low-energy magnon gap may be closed when the system is just at a quantum critical field that separates two different magnetic phases, where 2D gapless magnons would give $T^2$ dependence of *C*. However, we have resolved the gapless behavior in an extended field range of the



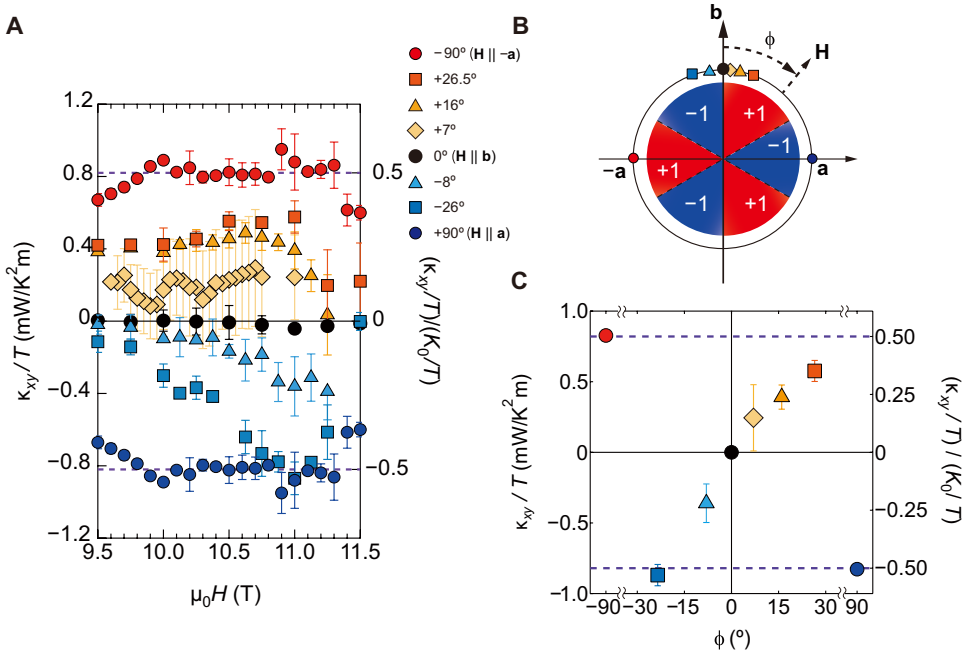


**Fig. 2. In-plane thermal Hall effect in the high-field quantum disordered phase of α-$RuCl_3$.** (**A**) Field dependence of $\kappa_{xy}/T$ at a temperature $T = 4.8$ K in the in-plane magnetic fields with different angles ϕ from the **b** axis. In the right axis, thermal Hall conductance is shown in units of the quantum thermal conductance $K_0 = (\pi^2/3)(k_B^2/h)T$. Dashed lines indicate the half-integer quantization. (**B**) In-plane field-angle dependence of the Chern number *Ch*. The same symbols are used as in **a** and **c** for the fixed field angles ϕ from the **b** axis. (**C**) Field-angle dependence of $\kappa_{xy}/T$ at a fixed field of 11 T at $T = 4.8$K.

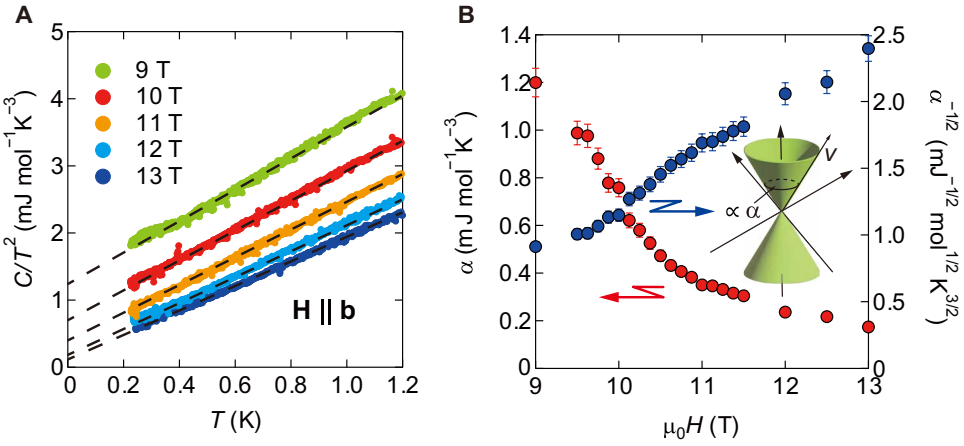


**Fig. 3. Specific-heat evidence of gapless excitations in the high-field phase of α-$RuCl_3$ for the bond-direction fields.** (**A**) Raw data of the temperature dependence of $C/T^2$ for **H**||**b** at several fields below 1.2 K. The linear fitting curves (dashed lines) resolve the residual $T$-linear term of $C/T$ ($\lim_{T\to 0} C/T = \alpha T$). (**B**) Field dependence of residual term α of $C/T^2$ (red circles). The right axis shows $\alpha^{-1/2}$ (blue circles), which is proportional to the Fermi velocity $v$ in the Dirac dispersion of gapless Majorana excitations (inset).

disordered phase above the antiferromagnetic critical field (~8 T), which indicates that the gap closure is not an accidental phenomenon but an intrinsic feature for the bond-direction fields as expected for the Majorana excitations in the KSL. The field dependence of α in the disordered phase shows a decreasing trend, which corresponds to the quasi-linear field dependence of Dirac velocity $v$ of the itinerant Majorana fermions (Fig. 3B). This appears to be related to the effective enhancement of the Kitaev interactions with increasing field (*31*), although the quantitative understanding of $v(H)$ requires further studies.

## DISCUSSION

Further evidence for the correctness of the Majorana-fermion description can be obtained in the angular dependence of low-temperature specific heat near the bond direction. When the field is slightly inclined from the **b** axis, we find a deviation from the $T$-linear behavior of low-temperature $C/T^2$. Such a deviation is found similarly for both $\phi < 0°$ (Fig. 4A) and $\phi > 0°$ (Fig. 4B). This can be easily understood by the fact that the observed deviations at low temperatures come from the opening of the excitation gap $\Delta_M(\phi) \propto |\sin 3\phi|$, which is symmetric with respect to the **b** axis ($\phi = 0°$). To analyze the data quantitatively, we use the 2D model for energy dispersion $E = \sqrt{v^2|\mathbf{k}|^2 + \Delta_M(\phi)^2}$ for the non-phononic contribution. Then, the low-temperature specific heat is given by

$$C/T = \alpha T\left[1 - \frac{\mathcal{G}(\Delta_M/T)}{\mathcal{G}(\infty)}\right] + \beta T^2, \mathcal{G}(y) \equiv \int_0^y \frac{dx}{2\pi}\frac{x^3 e^x}{(e^x+1)^2} \qquad (1)$$

Here, we ignore the contribution of the $Z_2$ fluxes whose gap is much larger than the measurement temperature scale, and the $\beta T^2$ term represents the phonon contribution (*26*). The fitting gives a good agreement with the data as shown by the solid lines in Fig. 4 (A and B), with the angle-dependent gap values as demonstrated in Fig. 4 (C and D). These results obtained by the low-temperature specific heat measurements fill an important missing range in the previous higher-temperature measurements (*26*), providing thermodynamic evidence of the distinct angle-induced gap closure. The angle dependence of the gap can be consistently described by the expectations for the Majorana gap $\Delta_M(\phi) = \Delta_0|\sin 3\phi|$ with the amplitude of $\Delta_0 \approx 10$ K (Fig. 4C). For $\phi = 0°$ (**H**||**b**), the $C/T^2$ data do not show the deviation from the $T$-linear dependence down to the lowest temperature, setting the upper bound of Majorana gap as $\Delta_M(0°) \lesssim 0.2$ K. This energy scale is much smaller than the magnon gap of ~1 meV, consistently estimated from several experiments (*16*, *32*–*34*) and from spin wave model calculations (*26*). Thus, we can safely conclude that the low-energy excitations revealed by the low-temperature specific heat lie well inside the magnon gap. We also note that in the low-field antiferromagnetic phase, the contrasting angular dependence with minimum specific heat for **H**||**b** has been found (*26*), highlighting the peculiar feature of the KSL phase.

The obtained results of thermal Hall conductivity and specific heat, namely, the sign change of the $Ch = \pm 1$ chiral edge mode with the gap closure for **H**||**b** ($\phi = 0°$), are a signature of the topological phase transition in a fermionic system outlined in Fig. 1B, excluding the bosonic scenario in Fig. 1C. It should also be emphasized that this characteristic angle-dependent low-energy gap is not expected for the chiral phonon Hall effect. The combination of these measurements also demonstrates the bulk-edge correspondence of topological properties of Majorana fermion excitations; when the bulk excitations are gapped (gapless), the edge currents appear (disappear). Our results evidencing the fermionic case imply that the quantization of the thermal Hall conductivity must occur at low enough temperatures compared with the Majorana gap if the phonon decoupling and domain issues (*23*–*25*) are not at play. In our sample, the half-integer quantization plateau is observed for **H**||±**a** ($\phi = \pm 90°$) at a temperature of 4.8 K (Fig. 2A), which is considered high enough to neglect the phonon decoupling effect (*23*). For small angles ($|\phi| \lesssim 10°$), the Majorana gap is smaller than the measurement temperature scale for $\kappa_{xy}$ [$\Delta_M(\phi) \lesssim 4.8$ K] as shown in Fig. 4C, which is likely responsible for the suppressed $\kappa_{xy}/T$ values from the half-integer quantization (Fig. 2, A and C). Even without having the quantization phenomena, however, the remarkable coincidence between the bulk gap closure and the sign-changing in-plane thermal

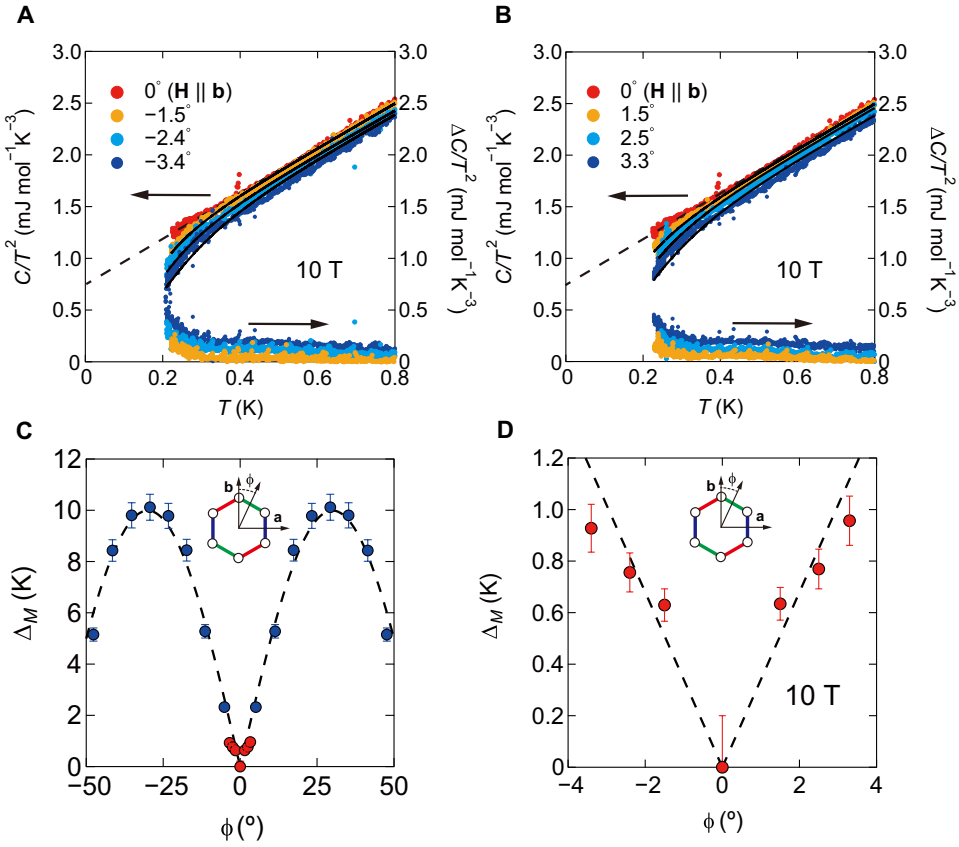


**Fig. 4. Rapid opening of the Majorana gap by tilting fields from the bond direction.** (**A** and **B**) Temperature dependence of $C/T^2$ at 10 T for negative (A) and positive (B) tilt angles ϕ from the bond direction (**b** axis). Dashed lines represent the linear fitting for ϕ = 0° and solid lines are fitting curves with the excitation gap $\Delta_M$ for finite angles. The data for the change in $C/T^2$ from ϕ = 0°, $\Delta C/T^2 = C(\phi = 0°)/T^2 - C(\phi)/T^2$, are also shown (right axis). (**C**) Angle dependence of Majorana gap $\Delta_M$ at 10 T. The data at low angles (red circles) are obtained in this study, which are compared with the high-angle data (blue circles) reported in the previous study in the temperature range down to 0.7 K (*26*). $\Delta_M(\phi)$ shows a |sin3ϕ| angle dependence (dashed lines). (**D**) The same data in the low-angle region. Errors in the Majorana gap are estimated from the uncertainties of fitting parameters. Inset shows the definition of ϕ.

Hall effect demonstrates that the topological transition of fermionic quasiparticles is induced by field angle rotation. From these results, we conclude that the excitations responsible for the planar thermal Hall effect in α-$RuCl_3$ are itinerant Majorana fermions in the KSL.

## MATERIALS AND METHODS

### Single crystals

High-quality single crystals of α-$RuCl_3$ were grown by the vertical Bridgman method (*35*). We used the same sample as in (*26*) for the specific heat measurements, in which the magnetic transition is seen only at 7 K, and no discernible anomaly is found at around 14 K associated with the stacking faults [see the magnetization data in figure S1 of (*26*)]. The orientation of the crystal axes is determined by x-ray diffraction measurements at room temperature.

### Measurement methods

The heat capacity measurements were performed by using the long-relaxation method in a Bluefors cryogen-free dilution refrigerator equipped with a superconducting magnet enabling $C(T)$ measurements at very low temperatures down to ~200 mK and in a magnetic field up to 13 T. The homemade cell was mounted on a two-axis rotator (attocube atto3DR), permitting to vary the angle three-dimensionally between the applied magnetic field and the sample.

Thermal conductivities were measured by a standard steady-state method by applying a temperature gradient along the crystallographic **a** axis. For thermal conductivity measurements, crystal #3 in (*12*), in which the half-integer–quantized thermal Hall effect is observed, was used. The direction of the crystal axes was determined by Laue x-ray back reflection measurements. The size of the crystal is 2150 μm (length) × (1000 ± 10) μm (width) × (20 ± 0.3) μm (thickness). Details of the measurement setups and procedures are described in the Supplementary Materials.

## Supplementary Materials

**This PDF file includes:**

Supplementary Text
Figs. S1 to S5
Tables S1 and S2
References

## REFERENCES AND NOTES

1. M. Sato, S. Fujimoto, Majorana fermions and topology in superconductors. *J. Phys. Soc. Jpn.* **85**, 072001 (2016).

2. A. Kitaev, Anyons in an exactly solved model and beyond. *Ann. Phys.* **321**, 2–111 (2006).
3. Y. Motome, J. Nasu, Hunting Majorana fermions in Kitaev magnets. *J. Phys. Soc. Jpn.* **89**, 012002 (2020).
4. G. Jackeli, G. Khaliullin, Mott insulators in the strong spin-orbit coupling limit: From heisenberg to a quantum compass and Kitaev models. *Phys. Rev. Lett.* **102**, 017205 (2009).
5. H. Suzuki, H. Liu, J. Bertinshaw, K. Ueda, H. Kim, S. Laha, D. Weber, Z. Yang, L. Wang, H. Takahashi, K. Fürsich, M. Minola, B. V. Lotsch, B. J. Kim, H. Yavaş, M. Daghofer, J. Chaloupka, G. Khaliullin, H. Gretarsson, B. Keimer, Proximate ferromagnetic state in the Kitaev model material $\alpha$-$RuCl_3$. *Nat. Commun.* **12**, 4512 (2021).
6. R. D. Johnson, S. C. Williams, A. A. Haghighirad, J. Singleton, V. Zapf, P. Manuel, I. I. Mazin, Y. Li, H. O. Jeschke, R. Valenti, R. Coldea, Monoclinic crystal structure of $\alpha$-RuCl3 and the zigzag antiferromagnetic ground state. *Phys. Rev. B* **92**, 235119 (2015).
7. R. Yadav, N. A. Bogdanov, V. M. Katukuri, S. Nishimoto, J. van den Brink, L. Hozoi, Kitaev exchange and field-induced quantum spin-liquid states in honeycomb $\alpha$-$RuCl_3$. *Sci. Rep.* **6**, 37925 (2016).
8. A. Banerjee, P. Lampen-Kelley, J. Knolle, C. Balz, A. A. Aczel, B. Winn, Y. Liu, D. Pajerowski, J. Yan, C. A. Bridges, A. T. Savici, B. C. Chakoumakos, M. D. Lumsden, D. A. Tennant, R. Moessner, D. G. Mandrus, S. E. Nagler, Excitations in the field-induced quantum spin liquid state of $\alpha$-$RuCl_3$. *npj Quant. Mater.* **3**, 8 (2018).
9. Y. Kasahara, T. Ohnishi, Y. Mizukami, O. Tanaka, S. Ma, K. Sugii, N. Kurita, H. Tanaka, J. Nasu, Y. Motome, T. Shibauchi, Y. Matsuda, Majorana quantization and half-integer thermal quantum Hall effect in a Kitaev spin liquid. *Nature* **559**, 227–231 (2018).
10. M. Yamashita, J. Gouchi, Y. Uwatoko, N. Kurita, H. Tanaka, Sample dependence of half-integer quantized thermal Hall effect in the Kitaev spin-liquid candidate $\alpha$-$RuCl_3$. *Phys. Rev. B* **102**, 220404 (2020).
11. J. A. N. Bruin, R. R. Claus, Y. Matsumoto, N. Kurita, H. Tanaka, H. Takagi, Robustness of the thermal Hall effect close to half-quantization in $\alpha$-$RuCl_3$. *Nat. Phys.* **18**, 401–405 (2022).
12. T. Yokoi, S. Ma, Y. Kasahara, S. Kasahara, T. Shibauchi, N. Kurita, H. Tanaka, J. Nasu, Y. Motome, C. Hickey, S. Trebst, Y. Matsuda, Half-integer quantized anomalous thermal Hall effect in the Kitaev material candidate $\alpha$-$RuCl_3$. *Science* **373**, 568–572 (2021).
13. Y. Kasahara, S. Suetsugu, T. Asaba, S. Kasahara, T. Shibauchi, N. Kurita, H. Tanaka, Y. Matsuda, Quantized and unquantized thermal Hall conductance of the Kitaev spin liquid candidate $\alpha$-$RuCl_3$. *Phys. Rev. B* **106**, L060410 (2022).
14. H. Zhang, A. May, H. Miao, B. Sales, D. Mandrus, S. Nagler, M. McGuire, J. Yan, Sample-dependent and sample-independent thermal transport properties of $\alpha$-$RuCl_3$. *Phys. Rev. Mater.* **7**, 114403 (2023).
15. P. Czajka, T. Gao, M. Hirschberger, P. Lampen-Kelley, A. Banerjee, J. Yan, D. G. Mandrus, S. E. Nagler, N. Ong, Oscillations of the thermal conductivity in the spin-liquid state of $\alpha$-$RuCl_3$. *Nat. Phys.* **17**, 915–919 (2021).
16. P. Czajka, T. Gao, M. Hirschberger, P. Lampen-Kelley, A. Banerjee, N. Quirk, D. G. Mandrus, S. E. Nagler, N. P. Ong, Planar thermal Hall effect of topological bosons in the Kitaev magnet $\alpha$-$RuCl_3$. *Nat. Mater.* **22**, 36–41 (2023).
17. E. Lefrancois, G. Grissonnanche, J. Baglo, P. Lampen-Kelley, J.-Q. Yan, C. Balz, D. Mandrus, S. E. Nagler, S. Kim, Y.-J. Kim, N. Doiron-Leyraud, L. Taillefer, Evidence of a phonon Hall effect in the Kitaev spin liquid candidate $\alpha$-$RuCl_3$. *Phys. Rev. X* **12**, 021025 (2022).
18. P. A. McClarty, X.-Y. Dong, M. Gohlke, J. G. Rau, F. Pollmann, R. Moessner, K. Penc, Topological magnons in Kitaev magnets at high fields. *Phys. Rev. B* **98**, 060404 (2018).
19. D. G. Joshi, Topological excitations in the ferromagnetic Kitaev-Heisenberg model. *Phys. Rev. B* **98**, 060405 (2018).
20. L. E. Chern, E. Z. Zhang, Y. B. Kim, Sign structure of thermal Hall conductivity and topological magnons for in-plane field polarized Kitaev magnets. *Phys. Rev. Lett.* **126**, 147201 (2021).
21. E. Z. Zhang, L. E. Chern, Y. B. Kim, Topological magnons for thermal Hall transport in frustrated magnets with bond-dependent interactions. *Phys. Rev. B* **103**, 174402 (2021).
22. X.-Y. Song, T. Senthil, Translation-enriched Z2 spin liquids and topological vison bands: Possible application to $\alpha$-$RuCl_3$. arXiv: 2206.14197. https://arxiv.org/abs/2206.14197.
23. Y. Vinkler-Aviv, A. Rosch, Approximately quantized thermal Hall effect of chiral liquids coupled to phonons. *Phys. Rev. X* **8**, 031032 (2018).
24. M. Ye, G. B. Halász, L. Savary, L. Balents, Quantization of the thermal Hall conductivity at small hall angles. *Phys. Rev. Lett.* **121**, 147201 (2018).
25. T. Kurumaji, Symmetry-based requirement for the measurement of electrical and thermal Hall conductivity under an in-plane magnetic field. *Phys. Rev. Res.* **5**, 023138 (2023).
26. O. Tanaka, Y. Mizukami, R. Harasawa, K. Hashimoto, K. Hwang, N. Kurita, H. Tanaka, S. Fujimoto, Y. Matsuda, E.-G. Moon, T. Shibauchi, Thermodynamic evidence for a field-angle-dependent Majorana gap in a Kitaev spin liquid. *Nat. Phys.* **18**, 429–435 (2022).
27. K. Hwang, A. Go, J. H. Seong, T. Shibauchi, E.-G. Moon, Identification of a Kitaev quantum spin liquid by magnetic field angle dependence. *Nat. Commun.* **13**, 323 (2022).
28. R. Matsumoto, R. Shindou, S. Murakami, Thermal Hall effect of magnons in magnets with dipolar interaction. *Phys. Rev. B* **89**, 054420 (2014).
29. S. Koyama, J. Nasu, Field-angle dependence of thermal Hall conductivity in a magnetically ordered Kitaev-Heisenberg system. *Phys. Rev. B* **104**, 075121 (2021).
30. S. Widmann, V. Tsurkan, D. A. Prishchenko, V. G. Mazurenko, A. A. Tsirlin, A. Loidl, Thermodynamic evidence of fractionalized excitations in $\alpha$-$RuCl_3$. *Phys. Rev. B* **99**, 094415 (2019).
31. J. Nasu, Y. Kato, Y. Kamiya, Y. Motome, Successive Majorana topological transitions driven by a magnetic field in the Kitaev model. *Phys. Rev. B* **98**, 060416 (2018).
32. A. N. Ponomaryov, E. Schulze, J. Wosnitza, P. Lampen-Kelley, A. Banerjee, J.-Q. Yan, C. A. Bridges, D. G. Mandrus, S. E. Nagler, A. K. Kolezhuk, S. A. Zvyagin, Unconventional spin dynamics in the honeycomb-lattice material $\alpha$-RuCl3: High-field electron spin resonance studies. *Phys. Rev. B* **96**, 241107 (2017).
33. R. Hentrich, A. U. B. Wolter, X. Zotos, W. Brenig, D. Nowak, A. Isaeva, T. Doert, A. Banerjee, P. Lampen-Kelley, D. G. Mandrus, S. E. Nagler, J. Sears, Y.-J. Kim, B. Buchner, C. Hess, Unusual phonon heat transport in $\alpha$-RuCl3: Strong spin-phonon scattering and field-induced spin gap. *Phys. Rev. Lett.* **120**, 117204 (2018).
34. D. Wulferding, Y. Choi, S.-H. Do, C. H. Lee, P. Lemmens, C. Faugeras, Y. Gallais, K.-Y. Choi, Magnon bound states versus anyonic Majorana excitations in the Kitaev honeycomb magnet $\alpha$-$RuCl_3$. *Nat. Commun.* **11**, 1603 (2020).
35. Y. Kubota, H. Tanaka, T. Ono, Y. Narumi, K. Kindo, Successive magnetic phase transitions in $\alpha$−RuCl3: XY-like frustrated magnet on the honeycomb lattice. *Phys. Rev. B* **91**, 094422 (2015).
36. J. A. N. Bruin, R. R. Claus, Y. Matsumoto, J. Nuss, S. Laha, B. V. Lotsch, N. Kurita, H. Tanaka, H. Takagi, Origin of oscillatory structures in the magnetothermal conductivity of the putative Kitaev magnet $\alpha$-$RuCl_3$. *APL Mater.* **10**, 090703 (2022).
37. S. Y. Park, S. H. Do, K. Y. Choi, D. Jang, T. H. Jang, J. Schefer, C. M. Wu, J. S. Gardner, J. M. S. Park, J. H. Park, S. Ji, Emergence of the isotropic Kitaev honeycomb lattice with two-dimensional Ising universality in $\alpha$-$RuCl_3$. arXiv: 1609.05690. https://arxiv.org/abs/1609.05690.
38. Y. Nagai, T. Jinno, J. Yoshitake, J. Nasu, Y. Motome, M. Itoh, Y. Shimizu, Two-step gap opening across the quantum critical point in the Kitaev honeycomb magnet $\alpha$-$RuCl_3$. *Phys. Rev. B* **101**, 020414 (2020).
39. H. B. Cao, A. Banerjee, J.-Q. Yan, C. A. Bridges, M. D. Lumsden, D. G. Mandrus, D. A. Tennant, B. C. Chakoumakos, S. E. Nagler, Low-temperature crystal and magnetic structure of $\alpha$-$RuCl_3$. *Phys. Rev. B* **93**, 134423 (2016).


**Acknowledgments:** We thank S. Fujimoto, K. Hwang, T. Kurumaji, Y. Motome, S. Murakami, N. P. Ong, H. Takagi, M. O. Takahashi, M. Udagawa, and M. G. Yamada for fruitful discussions. **Funding:** This work was supported by CREST (JPMJCR19T5) from Japan Science and Technology (JST), Grants-in-Aid for Scientific Research (KAKENHI) (nos. JP23H01829, JP22H00105, JP22K18683, JP21H01793, JP21KK0242, JP20H02600, JP19H00649, JP19K03711, and JP18H05227), and Grant-in-Aid for Scientific Research on Innovative Areas "Quantum Liquid Crystals (no. JP19H05824) from Japan Society for the Promotion of Science. E.-G.M. was supported by the National Research Foundation of Korea under grants NRF-2019M3E4A1080411, NRF-2020R1A4A3079707, and NRF-2021R1A2C4001847. **Author contributions:** K.I., Y.Mi., Y.Y., K.H., and T.S. performed specific heat measurements and analyses. S.S., Y.K., and Y.Ma. performed thermal conductivity measurements. N.K. and H.T. provided single crystals. P.N., J.N., and E.-G.M. provided theoretical inputs. T.S., Y.Ma., and E.-G.M. supervised the project. T.S. wrote the manuscript with inputs from K.I., S.S., K.H., P.N., J.N., E.-G.M., and Y.Ma. All authors participated in the discussion. **Competing interests:** The authors declare that they have no competing interests. **Data and materials availability:** All data needed to evaluate the conclusions in the paper are present in the paper and/or the Supplementary Materials.

Submitted 17 August 2023
Accepted 6 February 2024
Published 13 March 2024
10.1126/sciadv.adk3539